Received: 10 May 2024 | Revised: 19 June 2024 | Accepted: 9 August 2024 | Published online: 14 August 2024

RESEARCH ARTICLE

Journal of Optics and Photonics Research
2026, Vol. 3(1) 84–99
DOI: 10.47852/bonviewJOPR42023396

BON VIEW PUBLISHING

Direct Calculations of the Dielectric and Optical Parameters of Some Compound Semiconductors: A Study Using the Lorentz Oscillator and Wemple-DiDomenico Models

S. Abboudy[1], K. Alfaramawi[1,*], L. Abulnasr[1] and Basma K. Hefny[1]

[1]*Department of Physics, Alexandria University, Egypt*

Abstract: The Lorentz single oscillator model is widely utilized to describe the electron-phonon interaction in solids. The use of this model to calculate the dielectric function and optical parameters of compound semiconductors represents a novel approach in materials science which may lead to develop new materials with tailored optical properties and consequently can offer vast applications in areas such as quantum computing and quantum information processing. This work presents direct calculations of the complex dielectric function and some optical parameters, such as refractive index, extinction coefficient, and reflectivity for some selected III–V and II–VI compound semiconductors using Lorentz oscillator model. The dielectric and optical dispersion parameters among the infrared and visible electromagnetic spectra follow the so-called Transmission-Absorption-Reflection-Transmission (TART) trend. The TART curve provides information about how a material interacts with light at different wavelengths, which is crucial for understanding and optimizing various optoelectronic devices. Moreover, dielectric loss functions such as loss tangent, surface energy loss function, and volume energy loss function are investigated. The refractive index dispersion is analyzed using Wemple-DiDomenico (W-D) single effective oscillator model and Sellmeier equation. The energy of the effective single oscillator (E_o) and the dispersion energy (E_d) are estimated.

Keywords: dielectric function, Lorentz oscillator model, compound semiconductors, reflectivity, refractive index, Wemple-DiDomenico model

1. Introduction

Compound semiconductors, with their diverse electronic properties and applications, have garnered significant attention in both academic and industrial research. Understanding their optical and electronic characteristics is paramount for optimizing their performance in various optoelectronic devices, including solar cells, lasers, and photodetectors. One of the fundamental parameters that define these properties is the dielectric function, which reflects the material's response to electromagnetic fields as a function of frequency [1]. The dielectric function, often decomposed into its real and imaginary parts, serves as a correlation between the macroscopic Maxwell's equations and the microscopic electronic structure of materials [2]. Through its analysis, researchers can extract valuable information about a semiconductor's optical behavior, such as the refractive index (n), reflectivity (R), extinction coefficient (k), and others. Moreover, the dielectric function allows for the determination of intrinsic material properties, including the dielectric loss factor, surface energy loss function (SELF), and volume energy loss function (VELF), which are crucial for understanding energy dissipation mechanisms and material stability.

Numerous studies of the dielectric function for various solid materials have been introduced. For instance, Deneuville et al. [3] explored optical and electrical properties of n-type ZnSe heteroepitaxial thin films through the frequency-dependent dielectric function. Asadi and Nourbakhsh [4] used the density functional theory to investigate the structural, electronic, linear, and nonlinear response properties of the zinc-blende ZnSe and ZnTe. Taya and Ironside [5] utilized the Kramers-Kronig transformation to compute the electric permittivity of vacuum in the presence of a strong constant electric field. Additionally, Kayani et al. [6] and Poonam et al. [7] examined the dielectric and magnetic properties of diluted magnetic semiconductors such as Ag-doped zinc oxide (ZnO) thin films and Ti-doped MgSe. Ibrahim et al. [8] and Rivero Arias et al. [9] focused on the temperature dependence of the dielectric function for GaAs and InSb. Okbi et al. [10] expanded the scope of electronic structure and optical properties to $In_xAl_{1-x}P$ ternary alloys. Efil et al. [11] focused on metal-insulator-semiconductor structures based on ZnO. Lohner et al. [12] investigated amorphous germanium properties through ion implantation. Dey et al. [13] and Feizollahi Vahid et al. [14] delved into the effects of doping and nanocomposite films on dielectric properties. Forouhi and Bloomer [15] as well as recently Ticha and Tichy [16] developed empirical correlations and formulations for the optical band gap and refractive index for some crystalline solids.

*Corresponding author: K. Alfaramawi, Department of Physics, Alexandria University, Egypt. Email: kalfaramawi@alexu.edu.eg

The Lorentz single oscillator model is a widely used approach to describe the electron-phonon interaction in solids. Further understanding of this model leads to gain insights into the behavior of charged particles in complex physical systems. Accordingly, it potentially develops new materials with tailored optical properties which offers vast applications in areas such as quantum computing and quantum information processing. Recent papers studied the electron-phonon interactions using the Lorentz single oscillator model in semiconductors, see for example, Li et al. [17] as well as Xu et al. [18].

The use of the Lorentz single oscillator model to calculate the dielectric function and related optical parameters of compound semiconductors represents a novel approach in materials science. In the present work, we employed the Lorentz single oscillator model to specify the dispersion of the real and imaginary complex dielectric function and some related optical dispersion parameters for several compound semiconductors. The nominated systems include GaAs, InSb, and GaSb as examples of III–V materials and ZnTe, CdTe, and ZnS as II–VI compounds. The calculations are carried out in a frequency range, from infrared (IR) to ultraviolet (UV) electromagnetic spectra. Furthermore, Wemple-DiDomenico (W-D) single oscillator model is used to extract additional parameters, including single oscillator energy, dispersion energy, optical moments, static refractive index, oscillator wavelength, and Sellmeier parameter.

2. Theoretical Background

2.1. The model

Assume a heavily doped n-type semiconductor with (*N*) electron concentration subjected to electromagnetic wave of angular frequency (ω). The interaction between a single electron and the lattice phonons is described by a single oscillator that vibrates under the influence of the electromagnetic wave considering the damping effect. The Lorentz single oscillator approach is used to study the behavior of such single charged harmonic oscillator [19]. As a result, the dielectric function of a semiconductor is dispersed with interacting electromagnetic wave frequency to real and imaginary parts.

The real part of the dielectric function (ε_r) is given by [20]:

$$\varepsilon_r(\omega) = 1 + \frac{Ne^2}{m\,\varepsilon_0}\,\frac{(\omega_0{}^2-\omega^2)}{(\omega_0{}^2-\omega^2)^2+\gamma^2\omega^2} \tag{1}$$

where N is the electron concentration, m is the electron effective mass, ε_0 is the dielectric constant of free space. The atomic natural frequency ω_0 and the oscillator damping constant γ are related by [20]:

$$\gamma = 0.1\omega_0 \text{ and } \omega_0 = \sqrt{\frac{Ne^2}{m\,\varepsilon_0(\varepsilon_s-1)}}$$

where ε_s is the electric permittivity of the host semiconductor. The natural frequency of the oscillator is thus affected by the electron concentration and varies from one semiconductor to other by the electron effective mass and electric permittivity of the host material.

The imaginary part of the dielectric function (ε_{img}) is given by [20]:

$$\varepsilon_{img}(\omega) = \frac{Ne^2}{m\,\varepsilon_0}\,\frac{\gamma\omega}{(\omega_0{}^2-\omega^2)^2+\gamma^2\omega^2} \tag{2}$$

Therefore, the direct calculations of the two parts of the dielectric function can be carried out using Equations (1) and (2).

2.2. The optical parameters

The frequency-dependent optical properties are related to the dielectric constants of the material. The refractive index of a material is an important parameter that measures its transparency to incident spectral radiation and can be given by [21]:

$$n(\omega) = \frac{1}{\sqrt{2}}\cdot\sqrt{\varepsilon_r+\left(\varepsilon_r^2+\varepsilon_{img}^2\right)^{\frac{1}{2}}} \tag{3}$$

Using the model equations of the dielectric constants (1) and (2), one can estimate the refractive index from Equation (3).

Another important optical parameter is the extinction coefficient which is a measure of how much light is attenuated in a material. This is given by the equation [21]:

$$k(\omega) = \frac{1}{\sqrt{2}}\cdot\sqrt{-\varepsilon_r+\left(\varepsilon_r^2+\varepsilon_{img}^2\right)^{\frac{1}{2}}} \tag{4}$$

Knowing the parts of the dielectric constant leads to estimate the extinction coefficient of a semiconductor from Equation (4).

Reflectivity is an optical property which is determined by the fraction of light that is reflected from a semiconductor and can be evaluated from the equation [21]:

$$R(\omega) = \frac{(n-1)^2+k}{(n+1)^2+k} \tag{5}$$

Equation (5), thus, is used to obtain the reflectivity of a semiconductor material with the aid of Equations (3) and (4) (which consequently are dependent on Equations (1) and (2)).

2.3. Dielectric loss functions

Due to the interactions between electromagnetic waves and the materials and the oscillation of the electron single oscillator, there must be an energy loss. The dielectric energy loss is described by three functions: dielectric loss tangent, SELF, and VELF.

Dielectric loss tangent or tan delta ($tan\ \delta$) is the tangent of the angle between the alternating field vector and the material's Loss component. It is given by [22]:

$$\tan\delta = \frac{\varepsilon_{img}}{\varepsilon_r} \tag{6}$$

SELF is the energy lost by an electron when it interacts with the surface of a material and is given by [22]:

$$SELF = \frac{\varepsilon_{img}}{(\varepsilon_r+1)^2+\varepsilon_{img}^2} \tag{7}$$

Table 1
The constants used to calculate the real and imaginary parts of the dielectric constant for the nominated semiconductors

Parameter	Value					
	InSb	GaSb	GaAs	CdTe	ZnTe	ZnS
m/m_o	0.014	0.041	0.067	0.11	0.2	0.3
e	1.6×10^{-19} C					
ε_0	8.85×10^{-12} F/m					

Figure 1

Relation between the real part of the dielectric function and angular frequency for some selected III–V and II–VI semiconductors (InSb, GaAs, GaSb, CdTe, ZnTe, and ZnS) at three values of electron concentrations

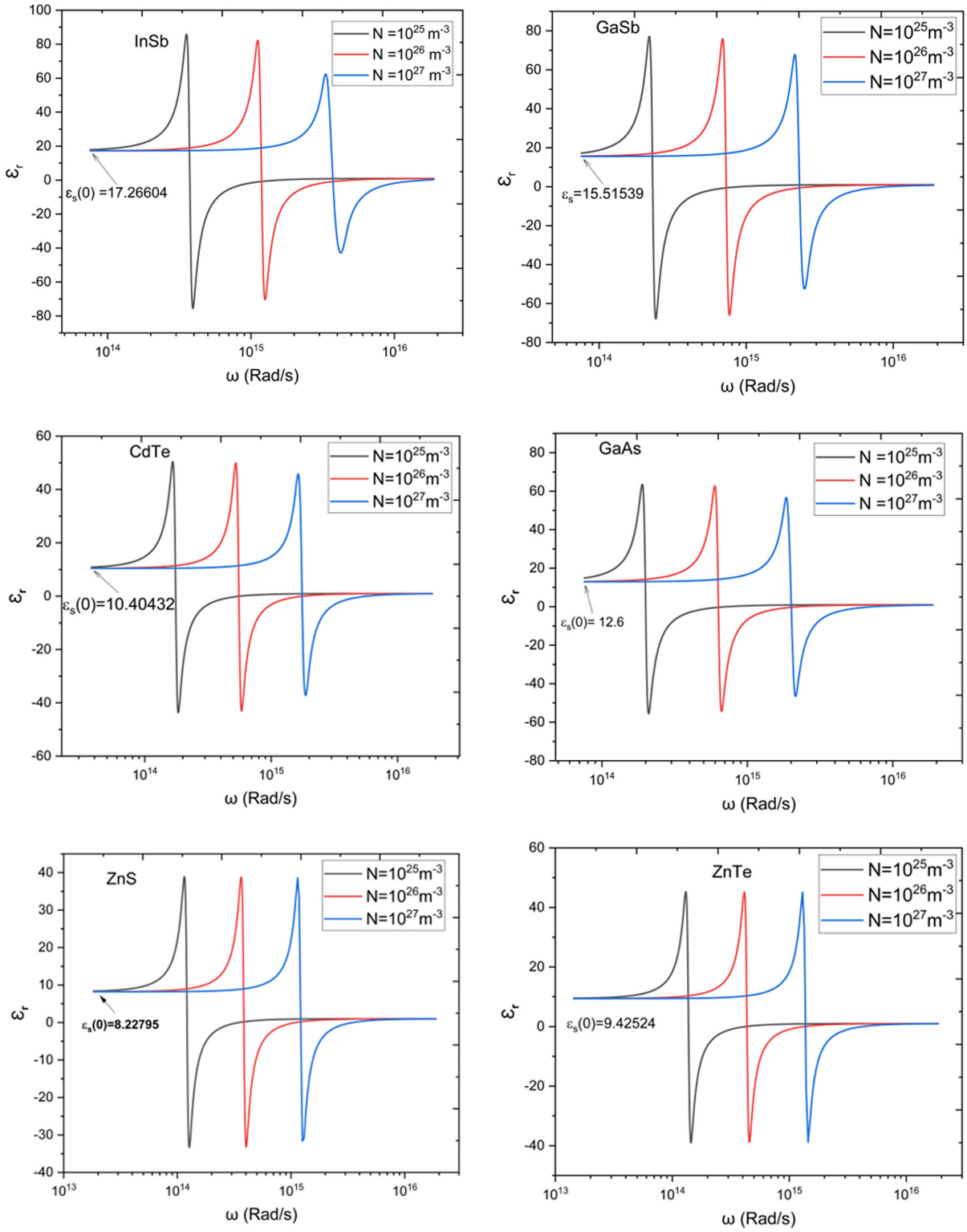

Table 2
Static dielectric constant, high-frequency dielectric constant, static refractive index, and the resonance frequency at three values of electron concentration extracted from Figures 1 and 2 for some III–V and II–VI compound semiconductors

Material	$\varepsilon_r(0)$	$\varepsilon_r(\infty)$	n_s	Resonance frequency ω_o (10^{14} rad/s)		
				$N = 10^{25}\ m^{-3}$	$N = 10^{26}\ m^{-3}$	$N = 10^{27}\ m^{-37}$
InSb	17.2	1	4.1	3.70	11.7	37.6
GaAs	12.6	1	3.5	2.00	6.28	19.8
GaSb	15.5	1	3.9	2.31	7.20	23.5
ZnTe	9.4	1	3	1.37	4.33	13.9
CdTe	10.4	1	3.2	1.76	5.50	17.0
ZnS	8.22	1	2.8	1.20	3.80	12.0

Figure 2
Relation between the imaginary part of the dielectric function and frequency for some selected III–V and II–VI semiconductors (InSb, GaAs, GaSb, CdTe, ZnTe, and ZnS) at three values of electron concentrations

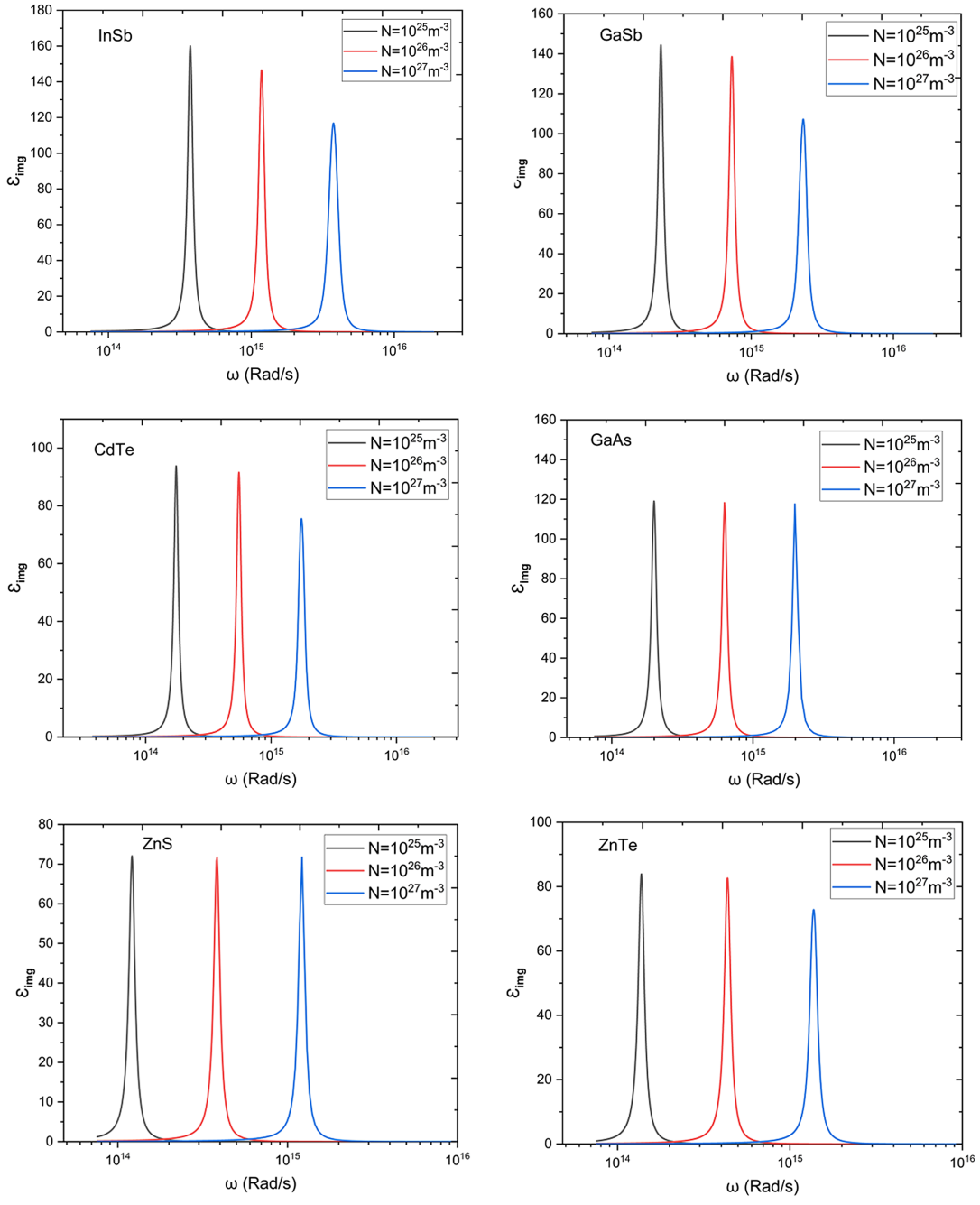

Figure 3

The refractive index as a function of photon frequency for some III–V compound semiconductors (InSb, GaSb, and GaAs) and II–VI compound semiconductors (CdTe, ZnTe, and ZnS) at different electron concentrations

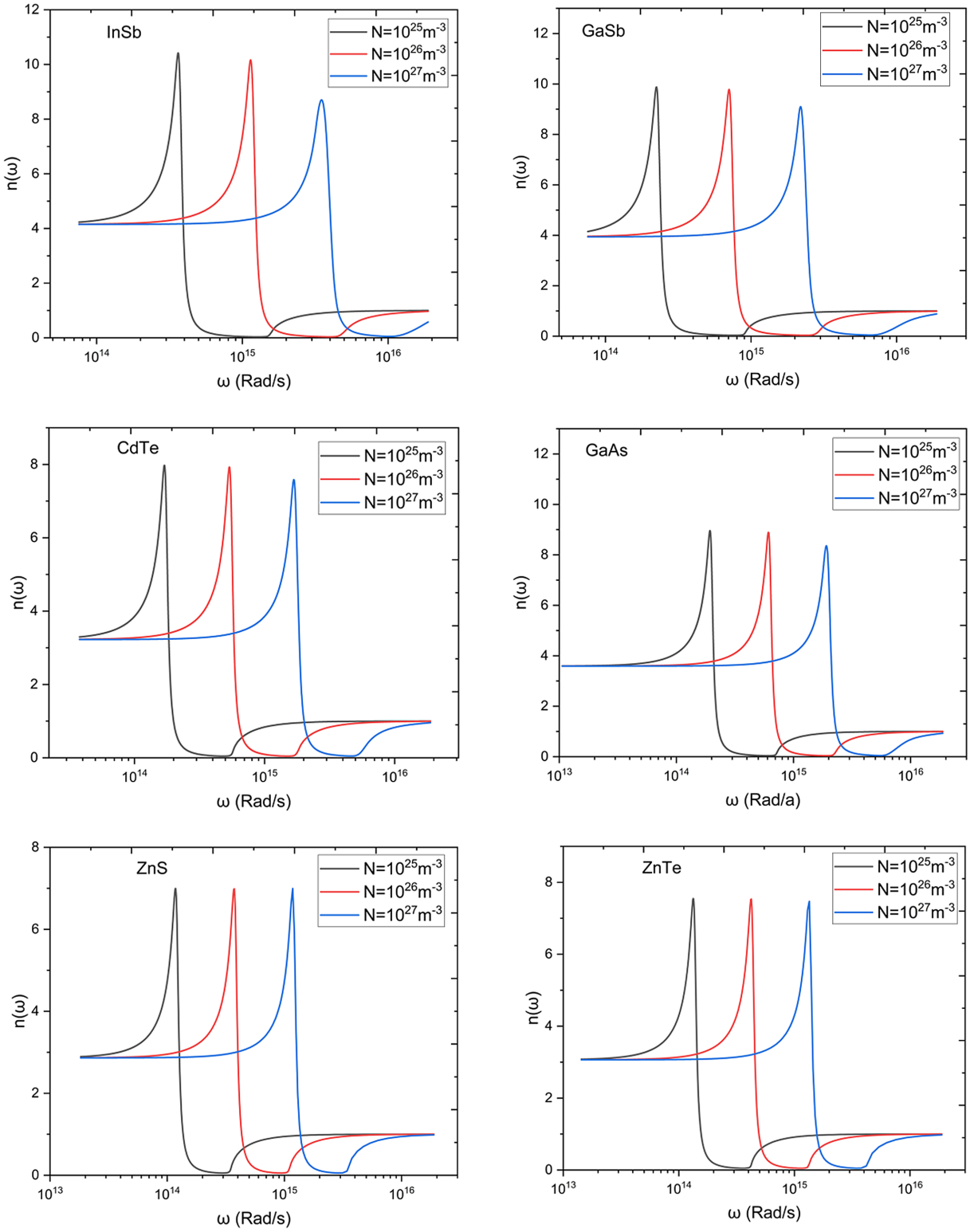

Figure 4

The extinction coefficient as a function of incident photon frequency for some III–V compound semiconductors (InSb, GaSb, and GaAs) and some II–VI compound semiconductors (CdTe, ZnTe, and ZnS) at different electron concentrations

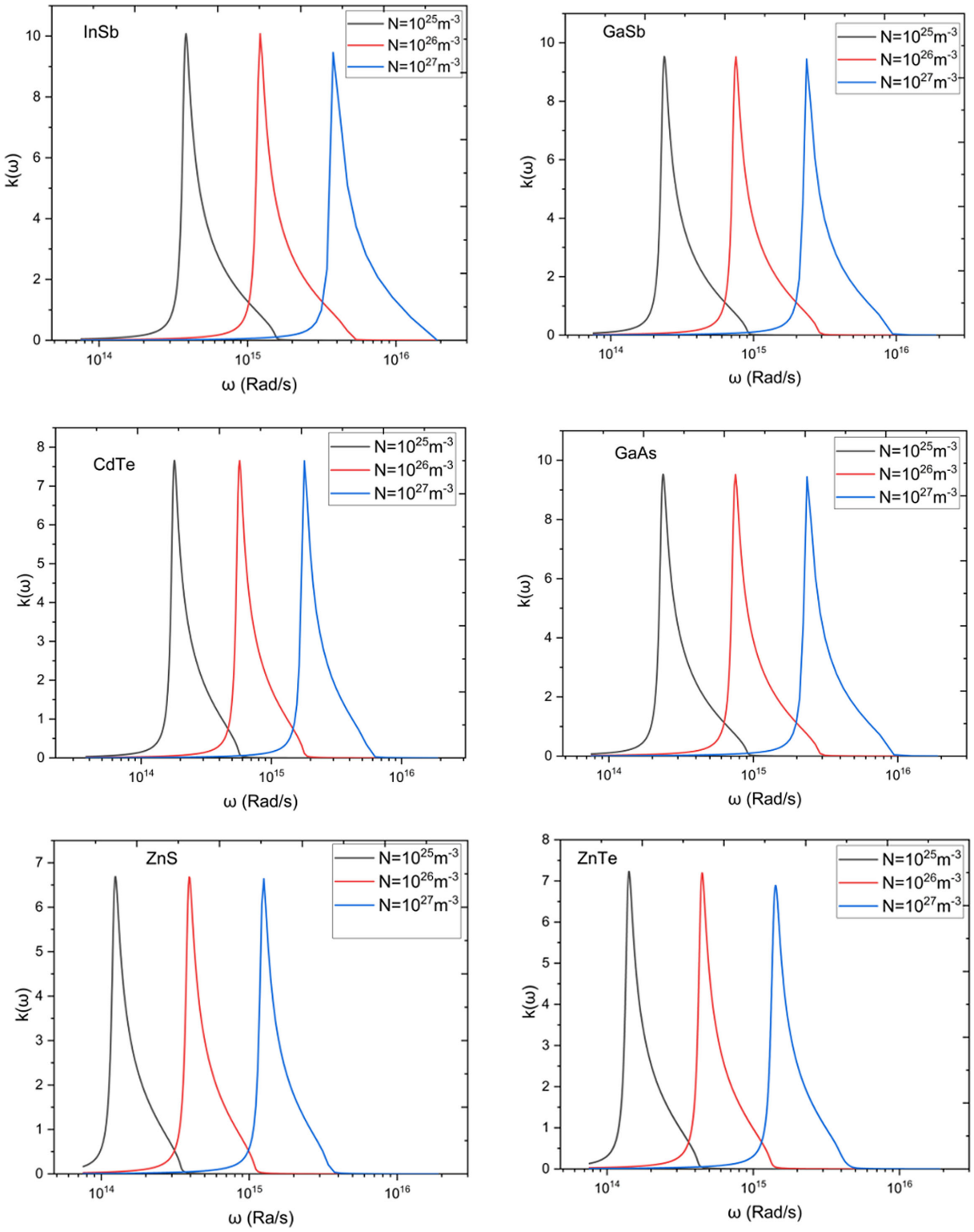

Figure 5
Reflectivity as a function of photon frequency for some selected III–V and II–VI compound semiconductors at different electron concentrations

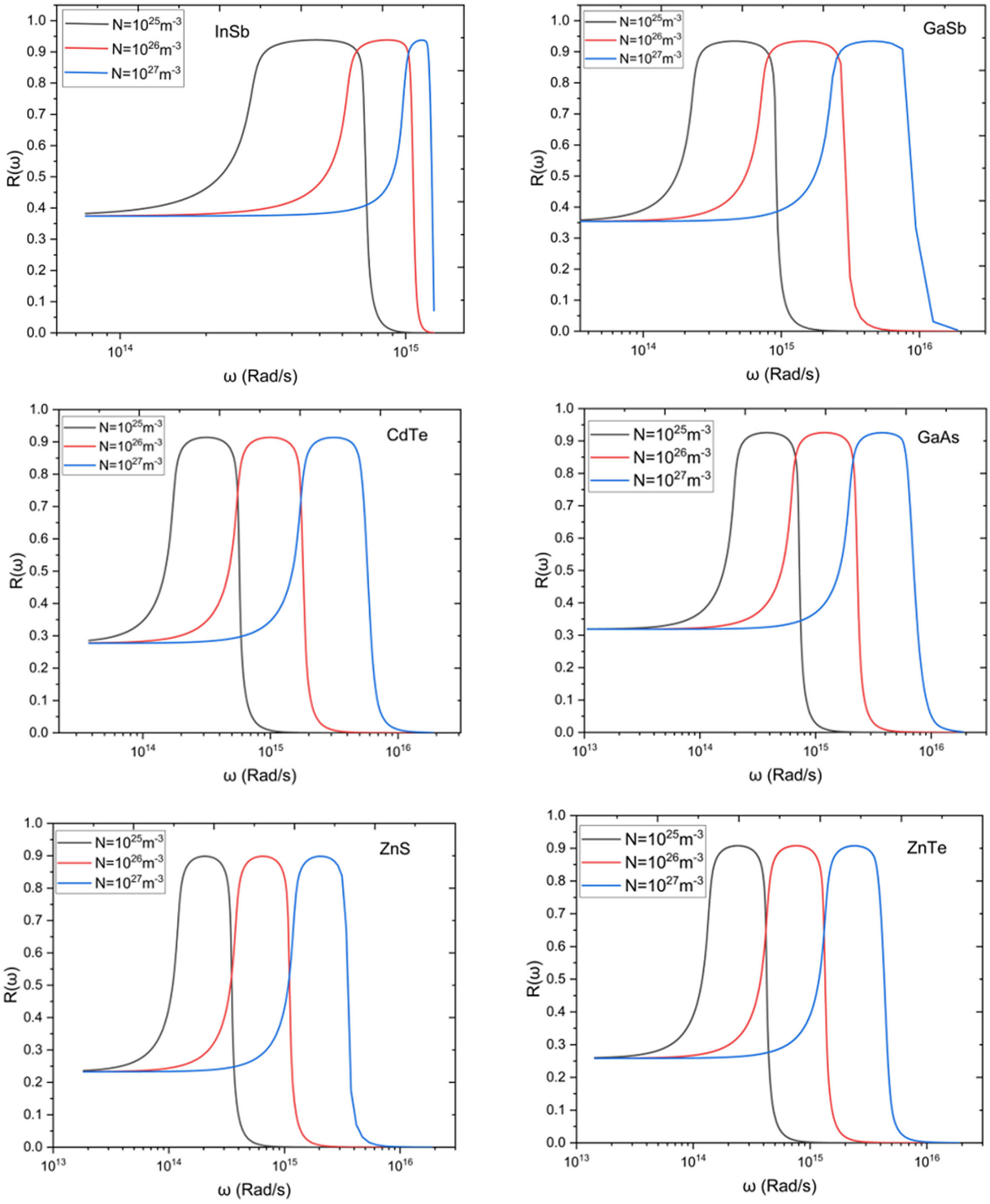

Figure 6
The two parts of the dielectric function and some optical parameters versus angular frequency of the electromagnetic waves for ZnS semiconductors

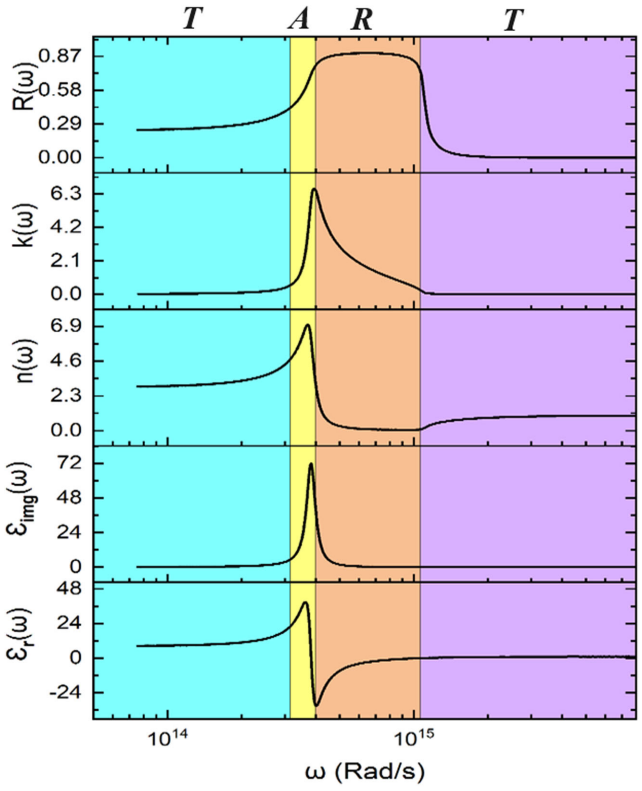

The VELF is a measure of the energy lost by an electron when it interacts with the bulk of a material [22]:

$$VELF = \frac{\varepsilon_{img}}{\varepsilon_r^2 - \varepsilon_{img}^2} \tag{8}$$

Therefore, the dielectric loss can be specified by Equations (6), (7), and (8) which use, of course, Equations (1) and (2).

2.4. W-D approach

The W-D approach [23] is important in analyzing the optical response of the material with free carriers. This model explores refractive index dispersion employing the single oscillator approximation which correlates the material's refractive index with the incident photon energy ($h\nu$) by the relation [24]:

$$\frac{1}{[n^2 - 1]} = \frac{E_0}{E_d} - \frac{1}{E_0 E_d} \cdot (h\nu)^2 \tag{9}$$

where E_o is the energy of the effective single oscillator and E_d is the dispersion energy, ν is the photon frequency and h Planck's constant. Equation (9) is used to determine the parameters E_o and E_d directly from the refractive index dispersion with photon energy.

The moments of the optical spectrum M_{-1} and M_{-3} are related to the effective single oscillator energy and dispersion energy and can be determined from the relations [23]:

$$E_0^2 = \frac{M_{-1}}{M_{-3}} \tag{10}$$

$$E_d^2 = \frac{M_{-1}^3}{M_{-3}} \tag{11}$$

On the other hand, the dispersion of the refractive index of the medium can be described by Sellmeier equation as a function of the incident photon wavelength as [25]:

$$n^2 = 1 + \frac{n_s^2 - 1}{\left[1 - \left(\frac{\lambda_o}{\lambda}\right)^2\right]} \tag{12}$$

where n_s is the static refractive index and λ_o is the average wavelength of the single oscillator. These parameters are related to the average oscillator strength S_0, or Sellmeier parameter, by the equation [26]:

$$S_0 = \frac{n_s^2 - 1}{\lambda_0^2} \tag{13}$$

3. Results and Discussion

3.1. Dielectric and optical dispersion parameters

Direct calculation of the real part of the dielectric constant as a function of angular frequency of the electromagnetic field is carried out using Equation (1). The constants used in these calculations are shown in Table 1 for some selected semiconductors.

In fact, Lorentz oscillator model is successfully applicable in metals with large electron concentrations where electron plasma is formed. As we tried to apply just model in semiconductors, we assumed doped materials having high carrier concentration. The values of the electron concentration are nominated to satisfy the condition of highly doped semiconductors which have electron densities greater than the critical ones estimated by Mott's criterion ($a_B n_c^{1/3} = 0.25$) where a_B is the effective Bohr radius of the semiconductor and n_c is the critical concentration. Many values were tried in the calculations, and we found that the best results are obtained at 10^{25} to 10^{27} m^{-3}. Figure 1 depicts the variation of the real part of the dielectric function with photon angular frequency for some selected III–V and II–VI semiconductors at three electron concentrations 10^{25}, $10^{26,}$ and 10^{27} m^{-3}. The trend of ε_r with photon frequency is the same for all semiconductors. At low ω, the real dielectric response is nearly constant and equals the static dielectric constant ε_s or $\varepsilon_r(0)$. Values of $\varepsilon_r(0)$ are estimated for the nominated compounds and listed in Table 2. These values are comparable to those reported in the literature. Increasing the frequency more led to an increase in ε_r until polarization catastrophe is occurred. Beyond this catastrophe, ε_r suddenly drops to a negative value, and with further elevation of ω, the dielectric constant starts to increase again till it reaches a saturation at the characteristic high-frequency dielectric constant $\varepsilon_r(\infty)$ or ε_∞. These values are estimated for all nominated semiconductors (see Table 2) and are found to be unity which agrees with the previously reported parameters in Lorentz oscillator model.

The imaginary part of the dielectric function with angular frequency for the same nominated semiconductors is illustrated in Figure 2 at different electron concentrations. The peak behavior of ε_{img} with photon frequency is recorded for all III–V and II–VI compound semiconductors. The maximum of the curve occurs at the characteristic resonance (or natural) frequency ω_o. These values are listed in Table 2. One can notice from Figure 2 that the resonance frequency increases as the electron concentration increases. Also, the peak height diminishes with rising of the electron concentration, and these are noticed for all semiconductor materials. When the electron

Figure 7
The tangent loss as a function of wave frequency for some III–V and II–VI compound semiconductors at different electron concentrations

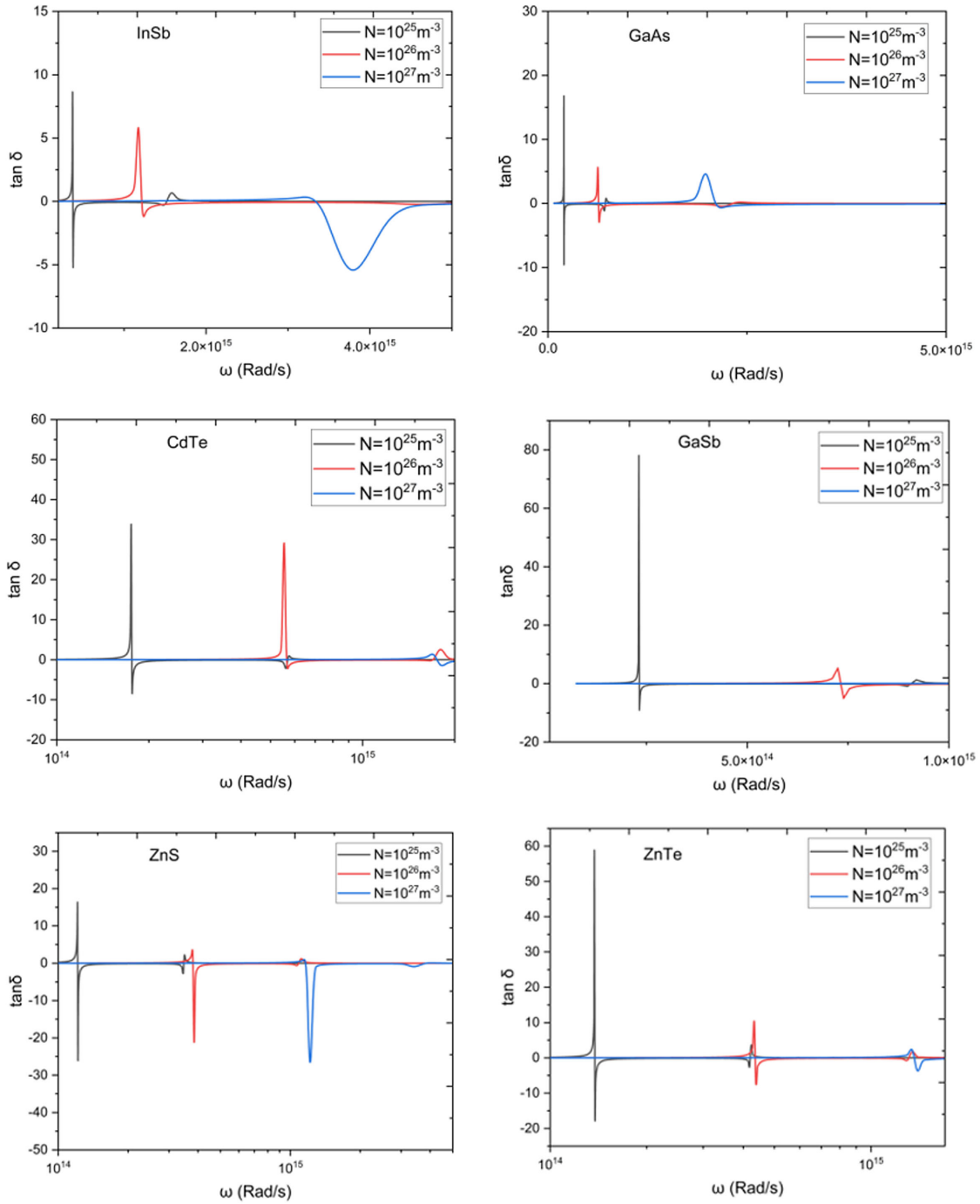

concentration increases, both the plasma frequency and the resonance frequency increase, and this will influence the material's optical properties. This finding can be attributed to the formation of plasmons due to large free carriers and thus excitations with optical spectra may lead to presence of photon polariton [27].

The refractive index is calculated using Equation (3) and by the aid of Equations (1) and (2). Figure 3 shows the behavior of refractive index $n(\omega)$ with incident photon angular frequency for the same selected semiconductors at three electron concentrations.

Figure 4 depicts the extinction coefficient $k(\omega)$ with ω for the same systems. The extinction coefficient is calculated from Equation (4), and the data are obtained from Equations (1) and (2). It is noticed from Figures 3 and 4 that the behavior of both refractive index and extinction coefficient with excitation photon frequency follows the peak trend for all nominated semiconductors. The position of the peaks is around the natural frequency and, consequently, varies with electron concentration. Additionally, at low frequencies, as the refractive index starts from a constant static value n_s, which is

Figure 8
The surface energy loss function (SELF) as a function of wave frequency for some III–V and II–VI compound semiconductors at different electron concentration

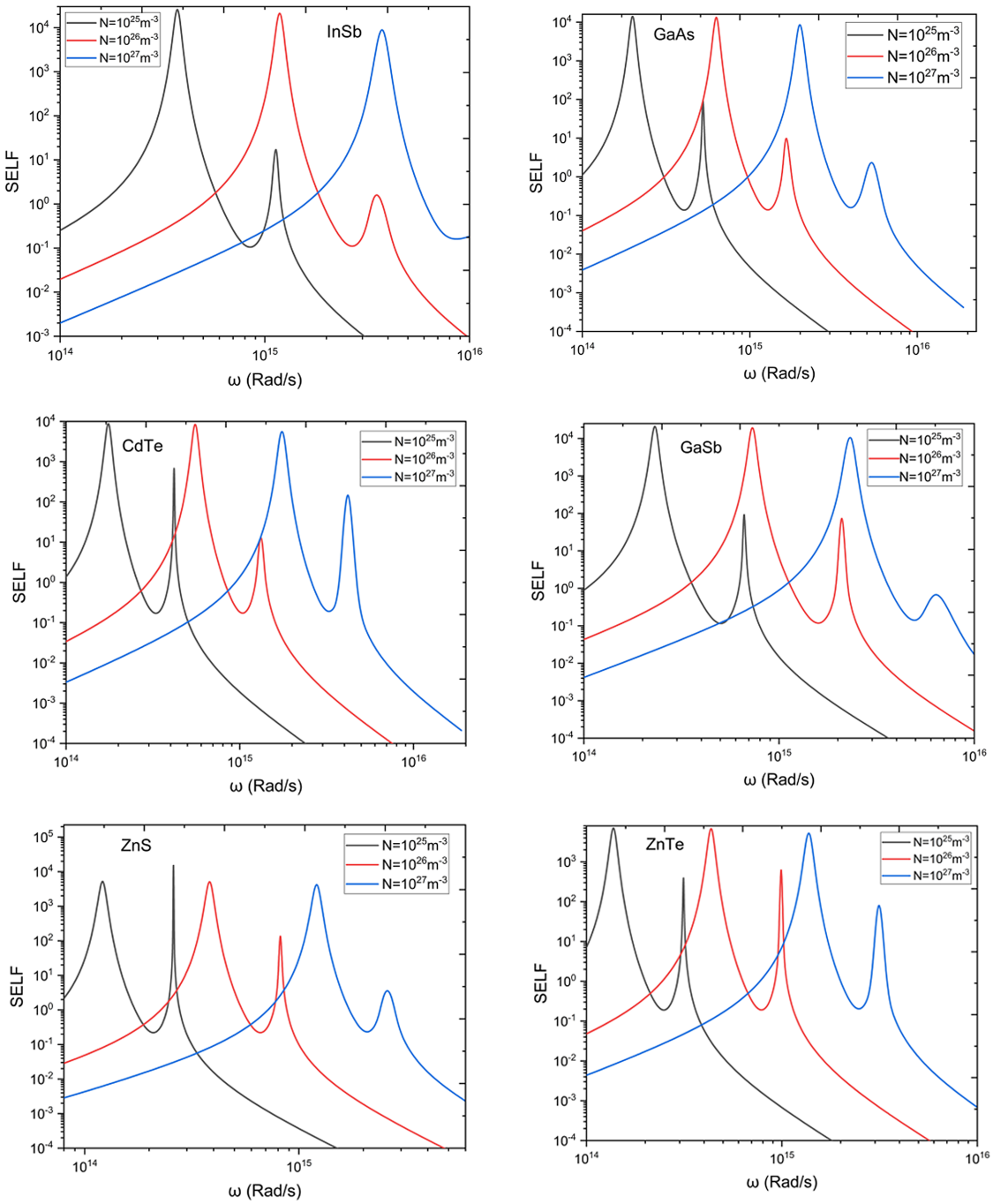

a characteristic parameter for each material (see Table 2), the extinction coefficient starts from nearly zero value. This is logically understood because the absorption of photons cannot take place in the beginning at the low-frequency range, only transmission can occur at this regime. By elevation of the photon frequency, both n and k increase monotonically due to the possibility of absorption as well as transmission of electromagnetic energy.

A higher value of $k(\omega)$ indicates an increase in the absorption of light at a particular frequency, which is crucial for understanding the material's performance in optoelectronic devices. These graphs not only demonstrate the frequency-dependent optical behavior of semiconductors but also serve as a foundation for designing and optimizing devices such as solar cells, photodetectors, and lasers.

Reflectivity is also calculated as a function of incident photon frequency for the selected semiconductors using Equation (5) and the results produced from Equations (3) and (4). Figure 5 demonstrates such a plot. These graphs demonstrate the material's ability to reflect incident light, which is essential for understanding its optical behavior and potential applications in reflective devices and coatings. The observed peaks and valleys in reflectivity signify

Figure 9
The volume energy loss function (VELF) as a function of wave frequency for some III–V and II–VI compound semiconductors at different electron concentrations

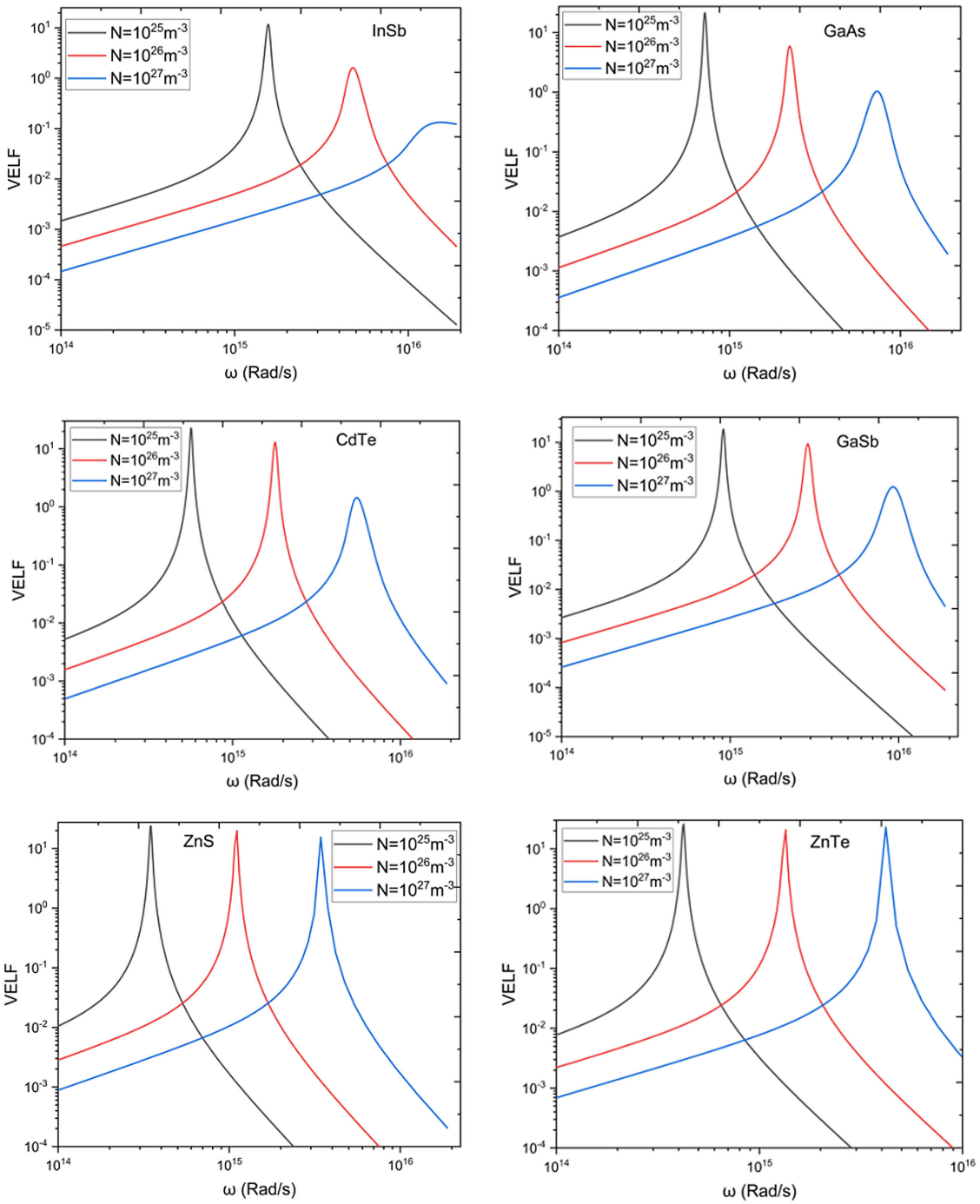

the material's interaction with light due to its electronic band structure, surface morphology, and composition. A higher reflectivity value indicates efficient reflection of light at specific frequencies, while lower values suggest increased absorption or transmission.

3.2. Transmission-Absorption-Reflection-Transmission (TART) analysis

The analysis of the optical parameters, through Figures 1 to 5, reveals the consistent behavior across all calculated parameters for the material using Lorentz oscillator model and its capability in semiconductors. Figure 6 summarizes the behavior of the dielectric and optical dispersion parameters for ZnS as an example. One can divide the behavior of these parameters among the IR and visible ranges of the electromagnetic spectra into four distinct regions known as TART analysis. The TART curve is an important tool for characterizing the optical properties of semiconductors. It provides information about how a material interacts with light at different wavelengths, which is crucial for understanding and optimizing various optoelectronic devices.

Table 3
The peak frequency for some III–V and II–VI compound semiconductors extracted from SELF and VELF figures at different concentrations

	Resonance frequency ω0 (10^{14} rad/s)					
	$N = 10^{25}$ m^{-3}		$N = 10^{26}$ m^{-3}		$N = 10^{27}$m^{-3}	
Material	SELF graphs	VELF graphs	SELF graphs	VELF graphs	SELF graphs	VELF graphs
InSb	3.76	15.7	11.7	47	37.6	120
GaSb	2.32	9.19	7.38	28.9	23.5	94
GaAs	1.9	7.2	6.2	22	19	75
ZnTe	1.36	4.18	4.38	13	13.95	41
CdTe	1.72	5.62	5.46	17	17.1	53
ZnS	1.2	3.45	3.8	11	12.1	34

Figure 10
***$(n^2–1)^{-1}$* as a function of *$(h\nu)^2$* for some nominated III–V and II–VI compound semiconductors at electron concentration of 10^{26} m^{-3}**

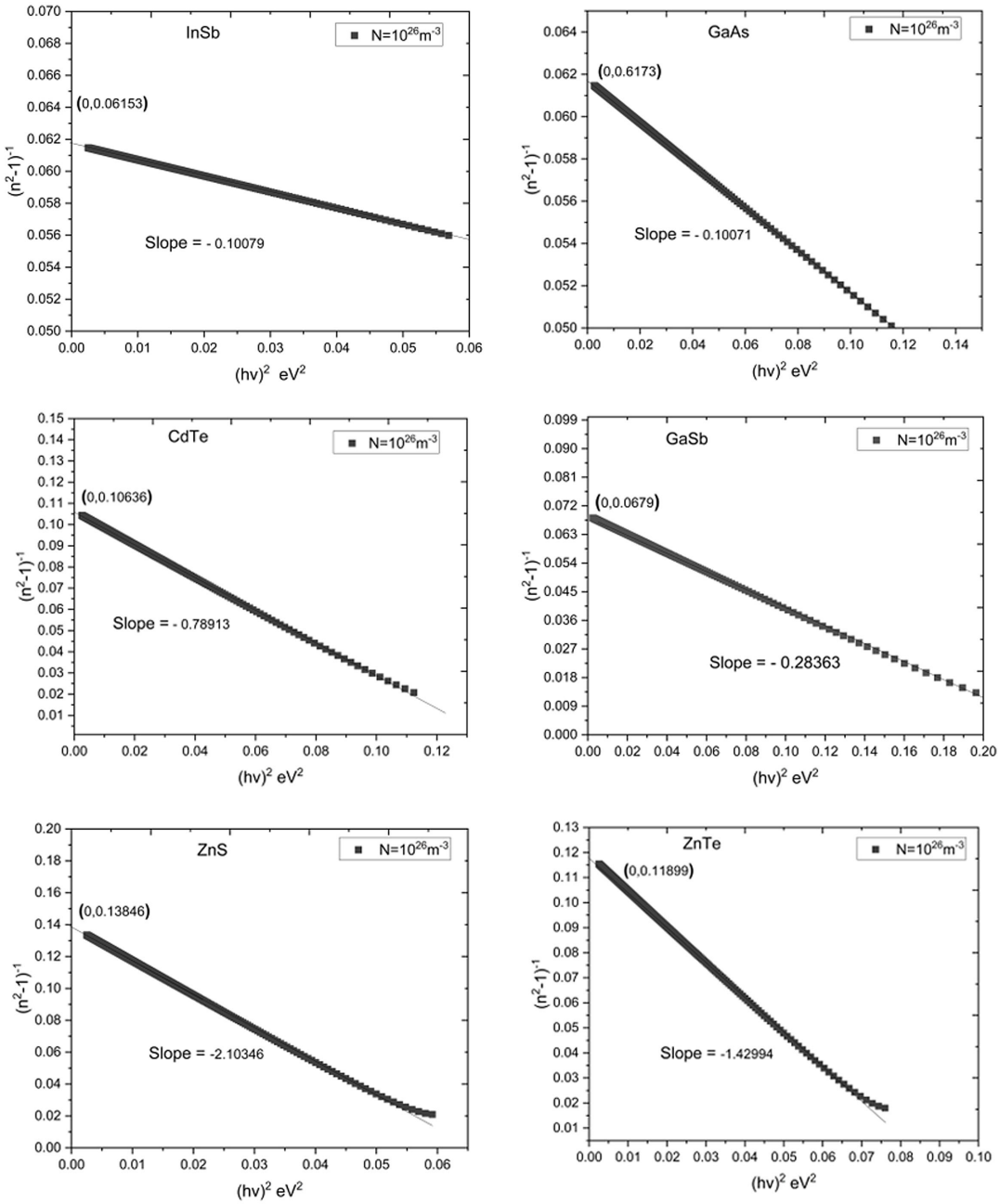

Table 4
Wemple-DiDomenico and Sellmeier single oscillator model parameters extracted from Figures 10 and 11 for some III–V and II–VI compound semiconductors at selected electron concentration

Parameter	InSb	GaSb	GaAs	ZnTe	CdTe	ZnS
E_0 (eV)	0.7813	0.489	0.7829	0.288	0.367	0.256
E_d (eV)	12.698	7.203	12.68	2.424	3.451	1.85
M_{-1}	16.243	14.8	12.682	8.4	9.407	1.85
M_{-3} $(eV)^{-2}$	26.628	61.99	20.69	101.0	69.89	28.15
n_s	4.148	3.943	3.595	3.0694	3.225	2.867
λ_0 (μm)	1.66	2.5	2.93	4.26	3.37	4.8
S_0 $(nm)^{-2}$	6.59×10^{-6}	2.3×10^{-6}	1.38×10^{-6}	4.62×10^{-7}	8.27×10^{-7}	3.13×10^{-7}

Figure 11
***$(n^2–1)^{-1}$* against *λ^{-2}* for some nominated III–V and II–VI compound semiconductors at electron concentration of 10^{26} m^{-3}**

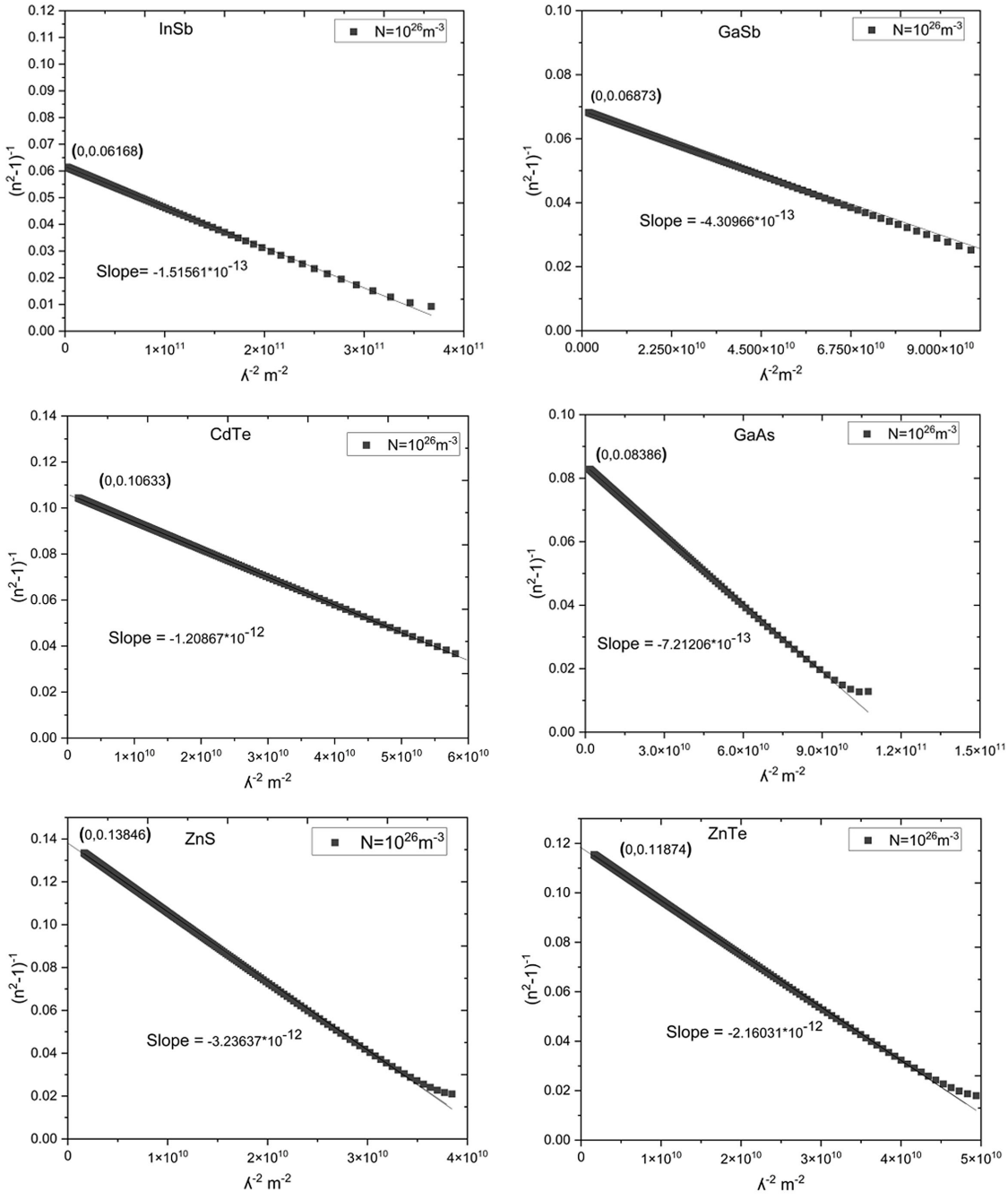

3.2.1. Initial transmission (T) phase

This phase lies in the IR spectrum which extends from frequencies less than 10^{13} Hz to about 5×10^{13} Hz. In this region, the energy of the incident photon is less than the semiconductor's energy gap E_g. Then, it may not promote electrons across the band gap. Consequently, the material remains transparent to these lower-energy photons, allowing light to traverse with minimal absorption or reflection. Therefore, this region is referred to as transmission (T) phase. In this phase, both components of the dielectric function, along with the optical parameters, increase as the frequency of the field rises.

3.2.2. Absorption (A) phase

This region starts from about 5×10^{13} Hz to about 6.5×10^{13} Hz, in the IR region. Absorption takes place when the photon energy of the incident wave matches or exceeds the bandgap energy E_g. Beyond a specific resonant frequency, electrons fail to synchronize with the wave, causing their motion to become out of phase. This leads to a sharp decline in permittivity, as depicted dramatically in Figure 6, defining the onset of anomalous dispersion or the so-called catastrophe. Maximum absorption is observed at $\omega = \omega_0$. The real dielectric function can assume negative values around resonances characterized by high losses. The width of this resonance is determined by the damping rate. Increasing γ leads to faster damping within a shorter duration. Other optical parameters also peak during this phase.

3.2.3. Reflection (R) phase

As already shown in Figure 6, in the frequency range from about 6.5×10^{13} Hz to 1.5×10^{14} Hz in the near IR regime, reflectivity attains its peak value, accompanied by a decline in other optical parameters. For instance, the refractive index diminishes due to electron absorption of photon energy.

3.2.4. Secondary transmission (T) phase

In the frequency range greater than 1.5×10^{14} Hz which includes near IR, visible, and UV spectra, materials exhibit negligible response at frequencies significantly above resonance, characterized by minimal losses. This behavior implies their transparency at extremely high frequencies.

3.3. Dielectric loss analysis

Dielectric loss in solids is described by tangent loss, SELF, and VELF. Equations (6), (7), and (8) are utilized to calculate such functions and by the aid of Equations (1) and (2). Figures 7, 8, and 9 show the relationship between these parameters and the photon angular frequency for the same selected semiconductors at three values of electron concentrations. The behavior of loss tangent with frequency, as recorded in Figure 7, is similar to the trend of the real part of the dielectric function. The loss is going through a maximum and then drops again.

On the other hand, it is demonstrated from Figures 8 and 9 that both SELF and VELF have peak behavior similar to that of the imaginary dielectric constant. It is noticed that the main peak at each concentration is located at the same resonance frequency mentioned above.

The resonance frequency for each semiconductor is extracted from Figures 8 (fundamental peak) and (9) at each electron concentration and listed in Table 3. The value extracted from SELF curve is generally smaller than that extracted from VELF curve. Consequently, the electrons lose their energies through traveling in the bulk of the material rather than through their propagation through the surface of the material. Generally, dielectric losses occur due to relaxation types of polarization. Therefore, dielectric losses are particularly high around the relaxation or resonance frequencies of polarization mechanisms. The polarization delays the applied field, resulting in an interaction between the field and the dielectric's polarization, leading to heating effects [28].

3.4. W-D dispersion analysis

Equation (9) of W-D approach can be explored through graphical representations by plotting $\frac{1}{[n^2-1]}$ against $(h\nu)^2$. Figure 10 shows such a plot for the investigated systems. This results in a linear relationship with a slope equivalent to $\frac{1}{E_0 E_d}$, and a y-axis intercept is given by $\frac{E_0}{E_d}$ from which one can determine the parameters E_0, E_d, M_{-1}, and M_{-3} using Equations (10) and (11). The values are listed in Table 4.

Furthermore, Sellmeier Equation (12) can be utilized by plotting $\frac{1}{[n^2-1]}$ against λ^{-2}, a straight line is obtained, its slope is $\frac{\lambda_0^2}{[n_s^2-1]}$, and the y-axis intercept equals $\frac{1}{[n_s^2-1]}$. Consequently, one can determine the oscillator strength and static refractive index from Equation (13) [29], see Figure 11. The calculated parameters are also given in Table 4. Values of n_s obtained here are very comparable with that given in Table 2.

4. Conclusions

Lorentz oscillator model is utilized to calculate the dielectric function and some related optical parameters for some nominated III–V and II–VI compound semiconductors in a frequency range from IR to UV electromagnetic spectra. The investigation revealed significant alterations in the real and imaginary parts of the dielectric function with the angular frequency. Results demonstrated that the electron concentration impacts both the resonance and plasma frequencies, affecting the optical characteristics. This is probably due to the formation of polaritons in these systems. The peaking behavior of dielectric loss at resonance frequencies is attributed to the relaxation polarization mechanisms. W-D single oscillator model and Sellmeier equation were used to extract additional parameters, including the single oscillator energy, dispersion energy, optical moments, static refractive index, oscillator wavelength, and Sellmeier parameter.

The frequency-dependent dielectric and optical behavior follows TART trend in the investigated frequency range. The TART curve analysis using the Lorentz oscillator model provides valuable insights into the optical properties of semiconductors, allowing researchers to better understand, characterize, and optimize these materials for a wide range of optoelectronic applications.

Ethical Statement

This study does not contain any studies with human or animal subjects performed by any of the authors.

Conflicts of Interest

The authors declare that they have no conflicts of interest to this work.

Data Availability Statement

Data are available from the corresponding author upon reasonable request.

Author Contribution Statement

S. Abboudy: Conceptualization, Methodology, Software, Validation, Formal analysis, Investigation, Resources, Data curation, Writing – original draft, Writing – review & editing, Visualization, Supervision, Project administration. **K. Alfaramawi:** Conceptualization, Methodology, Software, Validation, Formal analysis, Investigation, Resources, Data curation, Writing – original draft, Writing – review & editing, Visualization, Supervision, Project administration. **L. Abulnasr:** Conceptualization, Methodology, Software, Validation, Formal analysis, Investigation, Resources, Data curation, Writing – original draft, Writing – review & editing, Visualization, Supervision, Project administration. **Basma K. Hefny:** Software, Formal analysis, Investigation, Resources, Data curation, Writing – original draft.

References

[1] Johannesson, G., & Salem, N. (2022). Design structure of compound semiconductor devices and its applications. *Acta Energetica*, *46*(2), 28–35. https://actaenergetica.org/index.php/journal/article/view/466

[2] Tanner, D. B. (2019). *Optical effects in solids*. UK: Cambridge University Press. https://doi.org/10.1017/9781316672778

[3] Deneuville, A., Tanner, D. B., Park, R. M., & Holloway, P. H. (1991). Semiconductor electrical properties from the frequency dependence of the dielectric constant: Application to n-type ZnSe heteroepitaxial thin films. *Applied Surface Science*, *50*(1–4), 285–289. https://doi.org/10.1016/0169-4332(91)90183-K

[4] Asadi, Y., & Nourbakhsh, Z. (2019). First principle study of the structural, electronic, vibrational, thermodynamic, linear, and nonlinear optical properties of zinc-blende ZnSe and ZnTe semiconductors. *Computational Condensed Matter*, *19*, e00372. https://doi.org/10.1016/j.cocom.2019.e00372

[5] Taya, H., & Ironside, C. (2023). Kramers-Krönig approach to the electric permittivity of the vacuum in a strong constant electric field. *Physical Review D*, *108*, 096005. https://doi.org/10.1103/PhysRevD.108.096005

[6] Kayani, Z. N., Usman, A., Nazli, H., Sagheer, R., Riaz, S., & Naseem, S. (2020). Dielectric and magnetic properties of dilute magnetic semiconductors Ag-doped ZnO thin films. *Applied Physics A*, *126*(7), 559. https://doi.org/10.1007/s00339-020-03748-3

[7] Poonam, Saini, H. S., Thakur, J., Pundir, A. K., Singh, M., & Kashyap, M. K. (2019). Structural, electronic and magnetic properties of Ti-doped MgSe diluted magnetic semiconductor compound. *AIP Conference Proceedings*, *2093*(1), 020001. https://doi.org/10.1063/1.5097070

[8] Ibrahim, Z. A., Shkrebtii, A. I., Lee, M. J. G., Vynck, K., Teatro, T., Richter, W., …, & Zettler, T. (2008). Temperature dependence of the optical response: Application to bulk GaAs using first-principles molecular dynamics simulations. *Physical Review B*, *77*(12), 125218. https://doi.org/10.1103/PhysRevB.77.125218

[9] Rivero Arias, M., Armenta, C. A., Emminger, C., Zamarripa, C. M., Samarasingha, N. S., Love, J. R., …, & Zollner, S. (2023). Temperature dependence of the infrared dielectric function and the direct bandgap of InSb from 80 to 725 K. *Journal of Vacuum Science & Technology B*, *41*(2), 022203. https://doi.org/10.1116/6.0002326

[10] Okbi, F., Lakel, S., Benramache, S., & Almi, K. (2020). First principles study on electronic structure and optical properties of ternary semiconductor $In_xAl_{1-x}P$ alloys. *Semiconductors*, *54*(1), 58–66. https://doi.org/10.1134/S1063782620010182

[11] Efil, E., Kaymak, N., Seven, E., Tataroğlu, A., Ocak, S. B., & Orhan, E. (2019). Frequency dependent dielectric properties of atomic layer deposition grown zinc-oxide based MIS structure. *Physica B: Condensed Matter*, *568*, 31–35. https://doi.org/10.1016/j.physb.2019.05.016

[12] Lohner, T., Szilágyi, E., Zolnai, Z., Németh, A., Fogarassy, Z., Illés, L., …, & Fried, M. (2020). Determination of the complex dielectric function of ion-implanted amorphous germanium by spectroscopic ellipsometry. *Coatings*, *10*(5), 480. https://doi.org/10.3390/coatings10050480

[13] Dey, B., Narzary, R., Chouhan, L., Bhattacharjee, S., Parida, B. N., Mondal, A., …, & Srivastava, S. K. (2022). Crystal structure, optical and dielectric properties of Ag:ZnO composite-like compounds. *Journal of Materials Science: Materials in Electronics*, *33*(5), 2855–2868. https://doi.org/10.1007/s10854-021-07560-4

[14] Feizollahi Vahid, A., Alptekin, S., Basman, N., Ulusoy, M., Şafak Asar, Y., & Altındal, Ş. (2023). The investigation of frequency dependent dielectric properties and ac conductivity by impedance spectroscopy in the Al/(Cu-doped Diamond Like Carbon)/Au structures. *Journal of Materials Science: Materials in Electronics*, *34*(13), 1118. https://doi.org/10.1007/s10854-023-10546-z

[15] Forouhi, A. R., & Bloomer, I. (1988). Optical properties of crystalline semiconductors and dielectrics. *Physical Review B*, *38*(3), 1865–1874. https://doi.org/10.1103/PhysRevB.38.1865

[16] Ticha, H., & Tichy, L. (2023). Remark on the correlation between the refractive index and the optical band gap in some crystalline solids. *Materials Chemistry and Physics*, *293*, 126949. https://doi.org/10.1016/j.matchemphys.2022.126949

[17] Li, Z., Zhang, L., Zhou, Y., Zhang, H., Cheng, H., Meng, F., …, & Liu, Z. (2025). Modified Lorentz oscillator on modeling the dielectric function of Si and Ge. *The European Physical Journal Plus*, *140*(4), 293. https://doi.org/10.1140/epjp/s13360-025-06201-7

[18] Xu, M., Yang, J.-Y., Zhang, S., & Liu, L. (2017). Role of electron-phonon coupling in finite-temperature dielectric functions of Au, Ag, and Cu. *Physical Review B*, *96*(11), 115154. https://doi.org/10.1103/PhysRevB.96.115154

[19] Kuzmany, H. (2009). *Solid-state spectroscopy: An introduction*. Germany: Springer Science & Business Media.

[20] Han, F. (2012). *A modern course in the quantum theory of solids*. Singapore: World Scientific Publishing.

[21] Razeghi, M. (2006). *Fundamentals of solid state engineering*. USA: Springer.

[22] Abdullah, A. Q. (2013). Surface and volume energy loss, optical conductivity of rhodamine 6G dye (R6G). *Chemistry and Materials Research*, *3*(10), 56–63.

[23] Wemple, S. H., & DiDomenico, M. (1971). Behavior of the electronic dielectric constant in covalent and ionic materials.

Physical Review B, *3*(4), 1338–1351. https://doi.org/10.1103/PhysRevB.3.1338

[24] Borah, D. J., & Mostako, A. T. T. (2020). Investigation on dispersion parameters of Molybdenum Oxide thin films via Wemple–DiDomenico (WDD) single oscillator model. *Applied Physics A*, *126*(10), 818. https://doi.org/10.1007/s00339-020-03996-3

[25] Kompa, A., Lalitha Devi, B., & Chaitra, U. (2023). Determination of optical constants of vacuum annealed ZnO thin films using Wemple DiDomenico model, Sellmier's model and Miller's generalized rules. *Materials Chemistry and Physics*, *299*, 127507. https://doi.org/10.1016/j.matchemphys.2023.127507

[26] Alharthi, S. S., & Badawi, A. (2023). Modification of the structure and linear/nonlinear optical characteristics of PVA/Chitosan blend through CuO doping for eco-friendly applications. *Polymers*, *15*(10), 2391. https://doi.org/10.3390/polym15102391

[27] Inaoka, T. (1991). Plasmon-polar-phonon coupling at semiconductor surfaces. *Surface Science*, *257*(1–3), 237–258. https://doi.org/10.1016/0039-6028(91)90796-U

[28] Levitskaya, T. M., & Sternberg, B. K. (2019). *Electrical spectroscopy of earth materials*. Netherlands: Elsevier.

[29] Hassanien, A. S., Neffati, R., & Aly, K. A. (2020). Impact of Cd-addition upon optical properties and dispersion parameters of thermally evaporated $Cd_xZn_{1-x}Se$ films: Discussions on bandgap engineering, conduction and valence band positions. *Optik*, *212*, 164681. https://doi.org/10.1016/j.ijleo.2020.164681

How to Cite: Abboudy, S., Alfaramawi, K., Abulnasr, L., & Hefny, B. K. (2026). Direct Calculations of the Dielectric and Optical Parameters of Some Compound Semiconductors: A Study Using the Lorentz Oscillator and Wemple-DiDomenico Models. *Journal of Optics and Photonics Research*, *3*(1), 84–99. https://doi.org/10.47852/bonviewJOPR42023396